Energy Proceedings
Vol 52, 2025
ISSN 2004-2965

Characteristics and Key Controlling Factors of Impure CO_2 Huff-n-Puff and Storage in Shale Oil Reservoirs with Complex Fracture Networks

Lufei Bi[1], Jing Li[1*], Fuhao Guo[2], Shuyi Zhou[2]

1 National Key Laboratory of Petroleum Resources and Engineering, China University of Petroleum (Beijing), 102249, Beijing, China

2 College of Petroleum Engineering, China University of Petroleum (Beijing), Beijing 102249, China
(Corresponding Author: lijingsuc@163.com)

ABSTRACT

In the current context where the cost of obtaining pure CO_2 is high, using impure CO_2 gas for huff-n-puff is a more practical approach. The effects of impure CO_2 huff-n-puff and storage in shale reservoirs with complex fracture networks, as well as the characteristics and main controlling factors of injecting CO_2 of different purities for huff-n-puff and storage, are not yet well understood. This study considers the fracture extension mechanism in horizontal well fracturing and establishes an unstructured grid numerical model to depict fracture morphology. Using actual physical experiment results, a fluid model is fitted. By analyzing the impacts of huff-n-puff and storage under various production parameters and utilizing statistical methods, the key controlling factors of impure CO_2 huff-n-puff and storage in complex fracture well networks are identified and their characteristics are summarized. The results indicate that, compared to injecting pure CO_2 for huff-n-puff, injecting impure CO_2 can still significantly enhance the recovery rate of shale reservoirs. Furthermore, the effectiveness of huff-n-puff and storage increases with the enhancement of production parameters such as soaking time, injection rate, and cyclic cumulative injection rate. Among these factors, Injection rate has the greatest impact on huff-n-puff effectiveness, while the timing of huff-n-puff has the greatest impact on storage effectiveness. This research provides a robust theoretical foundation and practical guidance for improving the development efficiency of shale oil using impure CO_2 huff-n-puff technology.

Keywords: shale reservoirs, impure CO_2 huff-n-puff, complex fracture networks, CO_2 storage

1. INTRODUCTION

With the increasing global extraction and utilization of energy, energy issues have become more severe. An increasing number of unconventional oil and gas reservoirs are being developed, with shale reservoirs being a typical example of such unconventional resources. These reservoirs are characterized by ultra-low permeability, making it difficult to exploit them using conventional extraction technologies. Consequently, the development of shale reservoirs often involves the use of multi-fractured horizontal wells (MFHWs) (M. Zhang et al., 2024). This technology creates a Stimulated Reservoir Volume (SRV) around the well, which enhances the permeability of the shale and ultimately contributes to enhance oil recovery. Despite the implementation of MFHWs and other advanced extraction techniques, the inherent characteristics of shale reservoirs often lead to a rapid decline in initial production, followed by a period of low productivity. This decline necessitates the use of secondary recovery technologies to maintain stable production and further enhance oil recovery.

Gas injection, especially CO_2, is considere [1] d an effective EOR (Enhanced Oil Recovery) technology for unconventional reservoirs. CO_2 has advantages such as lower minimum miscibility pressure (MMP), making it the preferred choice for miscible gas EOR. Additionally, CO_2 exhibits higher injectivity and greater sweep efficiency. Moreover, CO_2 EOR can mitigate climate change through carbon capture, utilization, and storage. In the face of increasing challenges in global oil resource development, CO_2 huff-n-puff technology has gained widespread attention for its significant impact on enhancing oil recovery (Liang et al., 2024).

Currently, extensive physical experiments and numerical simulations have been conducted on CO_2 huff-n-puff technology (Shi et al., 2024; Wan et al., 2024; Y. Zhang et al., 2022). Typically, the CO_2 huff-n-puff process consists of three stages: injection, soaking, and production (M. Zhang et al., 2024). During the injection stage, CO_2 is introduced into the reservoir through the wellbore, initially permeating the fracture system and gradually penetrating the matrix system. This process supplements reservoir energy by pushing some of the oil from the matrix into the fractures and simultaneously

This is a paper for the 16th International Conference on Applied Energy (ICAE2024), Sep. 1-5, 2024, Niigata, Japan.

transporting oil deeper into the matrix (Yang et al., 2023). In the soaking stage, production from the well is closed, allowing the injected CO_2 to diffuse further into the reservoir (Lv et al., 2024). This diffusion helps equilibrate the pressure between the fractures and the matrix, enabling thorough contact between the oil and CO_2. Some of the CO_2 dissolves in the oil, causing the oil to swell and reducing its viscosity, while other portions of the CO_2 extract light hydrocarbons from the oil. During the production stage, CO_2 mobilizes and carries a portion of the oil through the fracture system to the wellbore, with some CO_2 remaining in the rock pores, achieving storage (Ren et al., 2024). However, current research primarily focuses on the application of pure CO_2. The potential of impure CO_2, particularly mixtures dominated by CH_4, in the huff-n-puff process remains relatively underexplored. Filling this research gap is crucial for advancing the oil and gas industry toward more innovative, flexible, and sustainable practices.

2. NUMERRICAL MODEL

2.1 Fluid phase behavior simulation

To accurately simulate the underground CO_2 huff-n-puff process, particularly in scenarios involving gas-liquid two-phase conditions, it is essential to model the fluid phase behavior precisely. In this study, the PVTi module of Eclipse was utilized to establish a compositional model, providing a robust fluid model for the gas injection numerical simulations. Based on field experimental data, the original formation fluid components were split and merged to enhance computational efficiency. The pseudo-components of the oil samples are detailed in Table 1, while Table 2 presents the key parameters obtained after fitting the formation fluid with Eclipse. The results demonstrate that the relative error between the experimental parameters and the numerical compositional model is within 5%, indicating high accuracy.

Table. 1 Pseudo-components of oil sample

Pseudo-component	CO_2	N_2	CH_4	C_2-C_5	C_6-C_{11}	C_{11}-C_{17}	C_{17+}
Molar composition	0.0179	0.0332	0.1303	0.1169	0.2791	0.2127	0.2099

Table. 2 Critical parameters of the compositional model

Pseudo-component	P_c, bar	T_c, K	Z_C	Omega A	Omaga B
CO_2	73.866	304.7	0.274	0.457	0.078
N_2	33.944	126.2	0.291	0.457	0.078
CH_4	46.042	190.6	0.285	0.457	0.078
C_{2+}	41.251	385.62	0.291	0.457	0.078
C_{6+}	26.056	592.49	0.249	0.457	0.078
C_{11+}	20.655	698.36	0.240	0.457	0.078
C_{17+}	10.756	955.36	0.225	0.457	0.078

2.2 Simulation of MMP

In high-temperature and high-pressure conditions, numerical simulations involving gas-liquid two-phase systems typically exhibit miscibility behavior, making the determination of MMP essential. This study establishes a slim tube simulation model based on experimental results. The slim tube, which is 20 meters long with a grid size of 50×1×1, measures 20m×0.0034m×0.0034m. Each end represents a production well and an injection well, as shown in Fig. 1. The experiment is conducted under constant temperature (94°C) with variable pressure conditions, demonstrating oil recovery rates when CO_2 gas is injected at different pressures. The MMP of the fluid, as determined by the slim tube simulation, is shown in Fig. 2.

As shown in Fig. 2, the pressure at which the oil recovery rate exhibits a noticeable inflection point is approximately 34.1 MPa, indicating the MMP. The numerical simulation results closely align with the physical experiment results, further confirming the reliability of the fluid model, which is suitable for subsequent CO_2 huff-n-puff numerical modeling. By comparing the simulated MMP with the reservoir pressure, it is evident that if the reservoir pressure exceeds the MMP, miscible displacement can be achieved under the current pressure conditions following gas injection into the formation.

Fig. 1 One-dimensional slim tube model

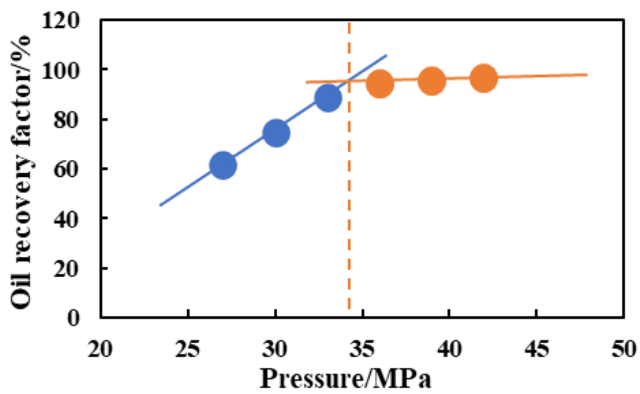

Fig. 2 The MMP for the slim-tube simulation

2.3 Numerical models considering complex fracture networks

For shale reservoirs, large-scale multistage fracturing of horizontal wells is often performed to modify the reservoir and establish an SRV, creating a complex fracture network around the wellbore. In such cases, conventional rectangular grids struggle to represent the complex fracture network morphology and cannot effectively differentiate between the matrix and the fractures, thereby weakening the influence of artificial fractures on fluid flow within the reservoir. Therefore, this study combines field logging data with simulations of the actual fracturing process in horizontal wells, considering the real pumping process and fracture propagation mechanisms. Based on the simulated discrete fracture network, a local unstructured grid model is established to accurately represent the true fracture morphology, enabling precise simulation of fluid flow between the matrix and artificial fractures. This approach helps develop an MFHWs model that accounts for complex fracture networks. The basic parameters of the reservoir and well are shown in Table 3.

Table. 3 Basic parameters of reservoir, well and fluid

Parameter	Value	Parameter	Value
Model size, m×m×m	2300×1100×360	Average permeability of matrix, mD	0.008
Number of grids	23×11×20	Average permeability of fracture, mD	112.5
Average porosity, %	5	Horizontal well length, m	1600
Reservoir depth, m	4057	Initial reservoir pressure, MPa	57

2.3.1 Numerical model gridding

Using well logging data interpolation, a basic property model was constructed. The logging interpretation results indicate that the average permeability of the matrix zone is 0.008 mD, while the average permeability of the fracture zone is 112.5 mD. The average porosity of the reservoir is 5%. To enhance computational efficiency, rectangular grids are used to represent the matrix system in the far-well region, while unstructured grid refinement is applied to characterize the fracture system near the wellbore. To avoid the impact of reservoir boundaries on fluid flow, the simulation model dimensions are set to 2300m×1100m×360m, corresponding to length, width, and height. The matrix grid consists of 23×11×20 cells, with a grid size of 100m×100m×18m, and the vertical layering coefficient is set to 4m. Fig. 3 shows the 3D grid of the single well model, and Fig. 4 illustrates the unstructured grid model of the complex fracture network.

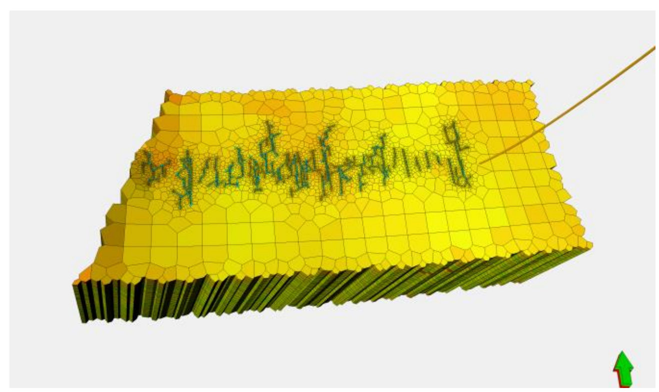

Fig. 3 The 3D grid of the well model

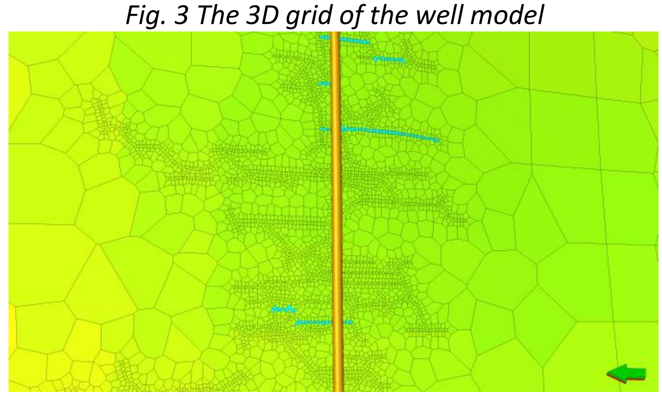

Fig. 4 The unstructured grid model of the complex fracture network

2.3.2 Matrix and fracture zone

To further distinguish between the matrix system and the fracture system, the model sets different relative permeability curves and rock compressibility coefficients for each system. It also uses grid equivalence and system partitioning to better characterize fluid transfer between the matrix and fractures. Additionally, the simulation of the pumping process enables the injection and presence of proppant, enhancing the accuracy of artificial fractures. The local fracture and matrix systems are shown in Fig. 5. Meanwhile, as production continues and the pressure wave propagates, the bottom-hole flowing pressure drops rapidly, causing strong stress sensitivity in the fracture area, which reduces the drainage area of the fractured horizontal well. To simulate this process, the model considers the stress sensitivity of the fractures, forming a reasonable pressure propagation pattern.

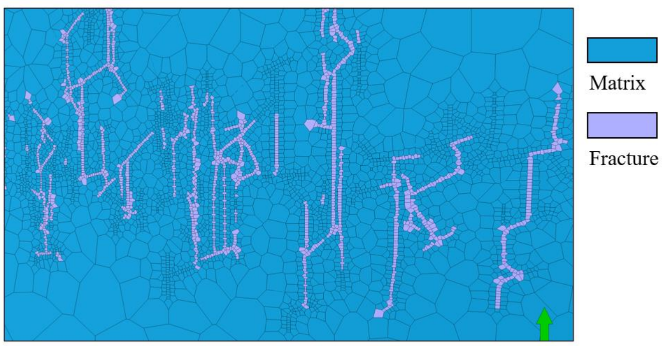

Fig. 5 The localized grid of fracture and matrix

2.3.3 Fluid data

The parameters used in this model are based on field-measured data from the oilfield, with a reservoir pressure of 57 MPa and a temperature of 94°C. The fluid model is incorporated into the numerical model, using equilibrium initialization to calculate parameters such as pressure at the reference depth and the oil-water contact depth, thereby establishing the fluid compositional model for the huff-n-puff process. By comparing the calculated reservoir pressure with the measured reservoir pressure and the model-calculated reserves with the proven geological reserves, the reliability of the numerical model is validated, with errors within 5%. This model can be used for subsequent production simulations.

2.3.4 Simulation accuracy analysis

To simulate real horizontal well fracturing production scenarios, a single well model underwent fracturing, water injection, well soaking, and flowback. Historical fitting results compared with actual production data showed high accuracy, allowing predictions for next-step production optimization schemes.

3. OPTIMIZATION OF INJECTIONE AND PRODUCTION PARAMETERS

After developing a numerical model that accounts for complex fracture networks, optimizing the CO_2 huff-n-puff injection and production parameters is crucial for effectively guiding field operations. This paper aims to explore the effects of different injection rates, timings, and CO_2 purities on huff-n-puff performance by comparing the results of various CO_2 injection scenarios. The objective is to identify the characteristics and key controlling factors of impure CO_2 huff-n-puff under complex fracture network conditions. This research seeks to provide effective guidance for unconventional oil and gas fields, enhancing oil recovery while also exploring the feasibility of CO_2 storage through the huff-n-puff process.

To verify the necessity of CO_2 huff-n-puff, cumulative oil production and oil exchange rate are used as evaluation indicators for huff-n-puff effectiveness, while the storage coefficient is used as an evaluation indicator for storage effectiveness. With other parameters kept constant, the total simulation period is set at 10 years to study the huff-n-puff and storage characteristics under different parameters. The specific design plan is shown in Table 4.

Table. 4 Parameters of the huff-n-puff

Simulation Case	Injection Timing	Injection Rate, $10^3m^3/d$	Huff-n-Puff Cycles	Gas Injection Time, d	Soaking Time, d	Production Time, y
Huff-n-Puff Injection of CO_2 with Different Purities After Initial Production	After 1 Year	20、30、40	4	180	30	1
	After 2 Years	20、30、40	4	180	30	1
	After 3 Years	20、30、40	4	180	30	1
	After 4 Years	20、30、40	4	180	30	1

3.1 Comparison of depleted production and CO_2 huff-n-puff production

First, simulations of depletion production and CO_2 huff-n-puff production were conducted. The depletion production involves continuous constant-pressure production for 10 years. For the CO_2 huff-n-puff simulation, constant-pressure production is carried out for 1 year, followed by 4 cycles of CO_2 huff-n-puff. The huff-n-puff process includes three stages: CO_2 injection, soaking, and constant-pressure production. Each huff-n-puff cycle is arranged as follows: gas injection for 180 days at an injection rate of 40,000 m^3/d, with an injection period of 180 days, followed by 30 days of soaking and 1 year of production.

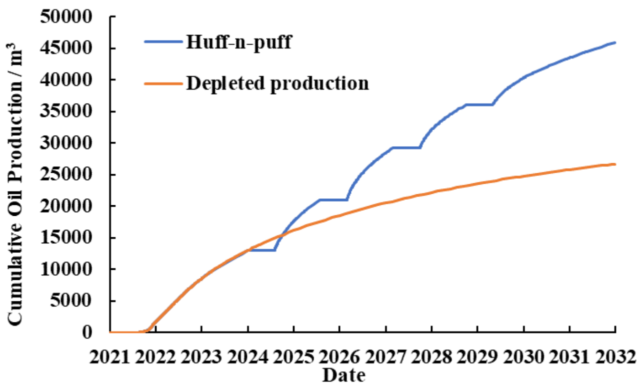

Fig. 6 Comparison of depleted production and CO_2 huff-n-puff production

Fig. 6 compares the cumulative oil production from depletion production and CO_2 huff-n-puff production. Relative to depletion production, CO_2 huff-n-puff technology enhances cumulative oil production. The injection of CO_2 elevates the average reservoir pressure, thereby supplementing the reservoir's energy and providing stability for subsequent production. Furthermore, the injected CO_2 dissolves in the crude oil, which increases the gas-oil ratio, leading to an expansion in the volume of crude oil and a reduction in its viscosity. These results demonstrate that CO_2 huff-n-puff technology can significantly improve the recovery of shale oil reservoirs.

3.2 Injection timing optimization

The timing of gas injection is determined by the production life, with four comparative scenarios established: CO_2 huff-n-puff after one, two, three, and four years of production. This setup is utilized to analyze the effects of varying injection timings on the oil recovery. The relationship between injection timing and cumulative oil production is illustrated in Fig. 7, while Fig. 8 depicts the inflection point in the decline of the oil exchange rate.

Comparing the simulation results of different injection timings, it is evident that the earlier the injection timing, the longer and more thoroughly the CO_2 contacts with the crude oil, resulting in higher cumulative oil production. Comparing the oil production increment ratio for different injection timings, it can be seen that there is little difference in the production increase effect when the injection occurs after 1, 2, or 3 years of production, with 3 years being the inflection point for enhanced production from CO_2 huff-n-puff. Additionally, the later the gas injection timing, the higher the CO_2 storage coefficient, resulting in better storage effectiveness. A lower reservoir pressure at the time of injection makes sequestration easier to achieve.

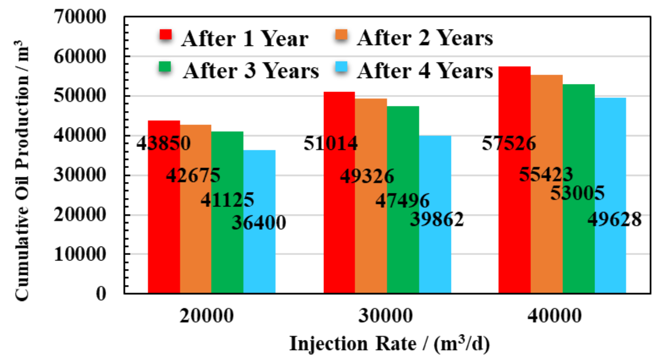

Fig. 7 Cumulative oil production with different timing of injection

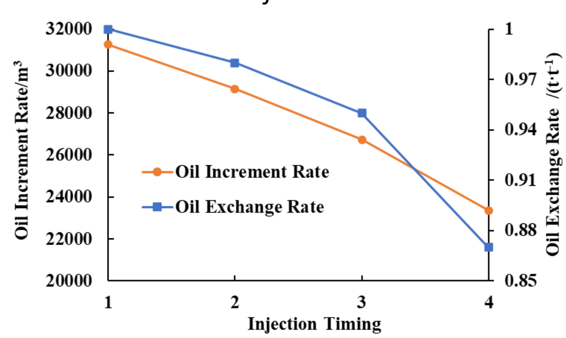

Fig. 8 Inflection point chart of decline in oil exchange rate

3.3 Injection rate optimization

Three groups of injection rates were established at 20,000 m^3/d, 30,000 m^3/d, and 40,000 m^3/d, respectively, to analyze the impact of varying gas injection rates on the recovery factor. The relationship between injection rate and cumulative oil production is illustrated in Fig. 9, while the inflection point of the decline in the oil exchange rate is depicted in Fig. 10.

Comparing the simulation results for different injection rates at the same gas injection timing reveals that as the injection rate increases, cumulative oil production continues to rise, while the oil exchange rate declines. Notably, the rate of decrease in the oil exchange rate diminishes once the injection rate exceeds 30,000 m^3/d. On one hand, a higher injection rate enhances the pressurization effect and improves reservoir energy replenishment. Conversely, if the injection rate is excessively high, the CO_2 may not have sufficient time to fully interact with the crude oil, potentially pushing the oil deeper into the matrix and complicating recovery efforts, which in turn slows the increase in cumulative oil recovery. Likewise, the storage coefficient rises with the CO_2 injection rate; however, beyond a certain threshold, the increase in the storage coefficient also decelerates, indicating an inflection point.

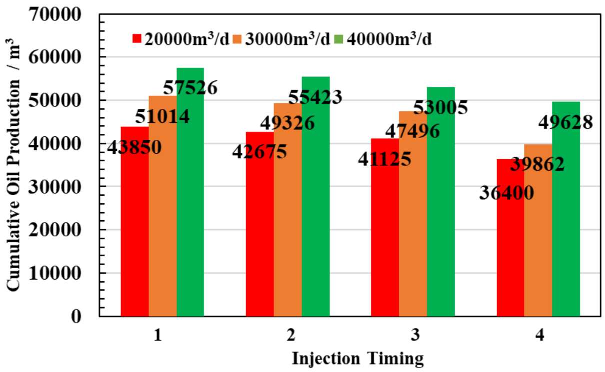

Fig. 9 Cumulative oil production for different injection rates

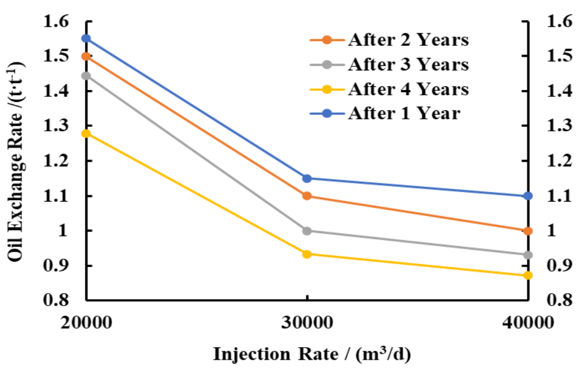

Fig. 10 Oil exchange rate chart for different injection rates

3.4 Comparison of huff-n-puff results with different CO_2 purities

To investigate the impact of different CO_2 purities on oil recovery, this study considers CH_4 as an impurity and designs six comparative scenarios with CO_2 purities ranging from 0 to 1. When the CO_2 purity is 1 and 0, it corresponds to pure CO_2 huff-n-puff and CNG huff-n-puff, respectively. It is evident that compared to CH_4, CO_2 has stronger solubility in crude oil, better expansion and viscosity reduction capabilities, and more easily achieves miscibility. As a result, the production enhancement effect of pure CO_2 huff-n-puff is superior to that of CNG huff-n-puff. The question arises: when CO_2 and CH_4 are mixed for injection, does a higher CO_2 purity always lead to better production enhancement? The comparison of cumulative oil production for different injection rates and different CO_2 purities is shown in Fig. 11, while the comparison for different injection timings and CO_2 purities is shown in Fig. 12.

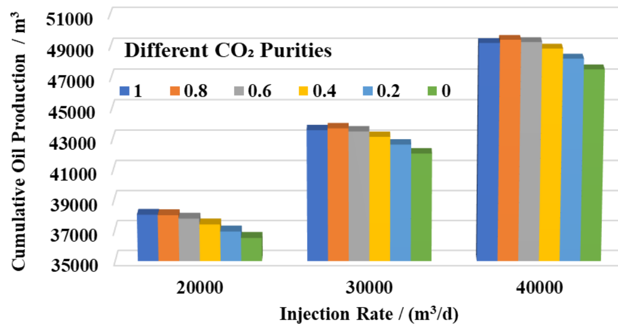

Fig. 11 Comparison of cumulative oil production results for different cases

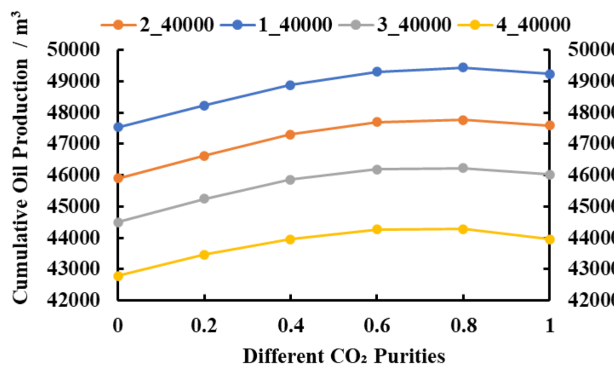

Fig. 12 Graph of cumulative oil production for different CO_2 purities

The results indicate that as the CO_2 purity increases, especially at high injection rates, the displacement type gradually transitions from non-miscible displacement to near-miscible and then to miscible displacement. The cumulative oil production gradually increases and reaches its peak within the 60%-80% purity range. This result suggests that for low-permeability reservoirs, injecting CO_2 mixed with CH_4 can better penetrate and displace the oil in low-permeability layers to achieve more effective displacement. Additionally, the CO_2 storage coefficient also increases with the increase in CO_2 purity. However, when the CO_2 concentration is too high, the increase in the storage coefficient slows down, indicating an optimal point.

4. ANALYSIS OF KEY CONTROL PARAMETERS

For the investigation of the main controlling factors in CO_2 huff-n-puff, this study employs the grey relational analysis (GRA) method. The principle of grey relational analysis is that it is a multi-factor statistical analysis method. In a grey system, this study aims to understand the relative strength of the influence of various factors on a particular item of interest. Specifically, it analyzes the degree to which each factor affects the item of interest. It assesses the degree of association between factors by evaluating the similarity in the geometric shape of their variation curves.

The results show that for the injection of impure CO_2 huff-n-puff, the production parameter with the greatest impact on production enhancement is the injection rate. The parameter with the greatest impact on storage effectiveness is the injection timing, followed by the injection purity.

5. CONCLUSIONS

This study systematically explored the huff-n-puff characteristics and main controlling factors of impure CO_2, a mixed gas with methane as the primary impurity, in unconventional reservoirs with complex fracture networks. The key conclusions of this study are as follows:

(1) Comparing the simulation results for different gas injection timings at the same injection rate, the earlier the gas injection timing, the earlier and more fully CO_2 can contact the crude oil, resulting in higher cumulative oil production. There is an inflection point for the production enhancement effect of gas injection timing. Additionally, the later the gas injection timing, the higher the CO_2 storage coefficient, resulting in better storage effectiveness.

(2) As the injection rate increases, the cumulative oil production continues to rise, while the oil exchange rate decreases with increasing injection speed. Once a certain injection rate is reached, the decrease in the oil exchange rate gradually levels off. The storage coefficient also increases with the CO_2 injection rate, but once the injection rate reaches a certain level, the increase in the storage coefficient will also slow down.

(3) Compared to CNG huff-n-puff, CO_2 has higher solubility and miscibility in crude oil, which provides better volume expansion and viscosity reduction effects, thereby making pure CO_2 huff-n-puff more effective than CNG huff-n-puff. Furthermore, for impure CO_2 huff-n-puff, especially with CH_4 mixed gas, there is significant potential to improve oil recovery. Studies show that as the CO_2 purity increases, cumulative oil production also significantly increases, particularly when CO_2 purity reaches 60%-80%, where the displacement effect is optimal. Therefore, this indicates that CO_2 mixed with CH_4 can better penetrate and displace oil in low-permeability reservoirs, thus achieving better production enhancement effects.

ACKNOWLEDGEMENT

This article was supported by the National Key Research and Development Program of China (2023YFB4104204) and the National Natural Science Foundation of China (51574257).

DECLARATION OF INTEREST STATEMENT

The authors declare that they have no known competing financial interests or personal relationships that could have appeared to influence the work reported in this paper. All authors read and approved the final manuscript.

REFERENCE.

[1] Liang, B., Chen, C., Jia, C., Wang, C., Wang, X., Zha, Y., Wang, R., Meng, Z., & Wang, H. (2024). Carbon capture, utilization and storage (CCUS) in oil and gas reservoirs in China: Status, opportunities and challenges. *Fuel*, *375*, 132353.

[2] Lv, W., Gong, H., Dong, M., Li, Y., Sun, H., Sun, Z., & Jiang, H. (2024). Potential of nonionic polyether surfactant-assisted CO_2 huff-n-puff for enhanced oil recovery and CO_2 storage in ultra-low permeability unconventional reservoirs. *Fuel*, *359*, 130474.

[3] Ren, Y.-J., Wei, B., Ji, B.-X., Pu, W.-F., Wang, D.-L., Tang, J.-Y., & Lu, J. (2024). Pore-scale probing CO_2 huff-n-puff in extracting shale oil from different types of pores using online T_1–T_2 nuclear magnetic resonance spectroscopy. *Petroleum Science*.

[4] Shi, Y., Wu, B., Wang, H., Li, Y., Liu, Z., Xu, C., Qin, J., Li, Y., Song, Z., & Liu, H. (2024). Insights into CO_2 huff-n-puff mechanisms from laboratory experiment and single-well pilot test in the Lucaogou tight oil reservoir, Jimsar sag, China. *Geoenergy Science and Engineering*, *232*, 212456.

[5] Wan, Y., Jia, C., Lv, W., Jia, N., Jiang, L., & Wang, Y. (2024). Recovery mechanisms and formation influencing factors of miscible CO_2 huff-n-puff processes in shale oil reservoirs: A systematic review. *Advances in Geo-Energy Research*, *11*(2), Article 2.

[6] Yang, Y.-L., Hu, Y., Zhu, Y.-T., Zhang, J.-G., Song, P., Qin, M., Wu, H.-R., Song, Z.-J., & Hou, J.-R. (2023). Similarity-based laboratory study of CO_2 huff-n-puff in

tight conglomerate cores. *Petroleum Science*, *20*(1), 362–369.
[7] Zhang, M., Li, B., Lei, W., Zhao, X., Ding, W., Zhang, X., Xin, Y., & Li, Z. (2024). Oil displacement and CO_2 storage during CO_2 immiscible huff-n-puff within a saturated reservoir: An experimental study. *Fuel*, *371*, 132026.
[8] Zhang, Y., Zou, Y., Zhang, Y., Wang, L., Liu, D., Sun, J., Ge, H., & Zhou, D. (2022). Experimental study on characteristics and mechanisms of matrix pressure transmission near the fracture surface during post-fracturing shut-in in tight oil reservoirs. *Journal of Petroleum Science and Engineering*, *219*, 111133.